CILAMCE 2017
Florianópolis - Santa Catarina - Brazil

NUMERICAL STUDY OF NON-NEWTONIAN FLUID FLOWS IN Y-SHAPED STRUCTURES

Alysson Sehn

Vinicius da Rosa Pepe

alysson.sehn@gmail.com

viniciuspepe@gmail.com

Graduate Program in Mechanical Engineering, Universidade Federal do Rio Grande do Sul

Rua Sarmento Leite, 425, 90050-170, Porto Alegre, RS, Brazil.

Antonio Ferreira Miguel

afm@uevora.pt

Department of Physics, School of Science and Technology, University of Evora

Largo dos Colegiais 2, 7000, 7000-049, Évora, EVR, Portugal

Flavia Zinani

Luiz Alberto Oliveira Rocha

fzinani@unisinos.br

laorocha@gmail.com

Graduate Program in Mechanical Engineering, Universidade do Vale do Rio dos Sinos

Av. Unisinos, 950, 93022-750, São Leopoldo, RS, Brasil

Abstract. *Vascular and respiratory trees are complex flow systems consisting of series of large and small ducts. Although the literature reports several cases that are in accordance with Hess-Murray law, there are also some branching patterns of natural systems that deviate from this law. In this study, a numerical analysis was carried out to investigate laminar fluid flow of non-Newtonian fluids, in Y-shaped flow structures with different ratios between the sizes of parent and daughter ducts. The non-Newtonian behavior was modeled using the power-law equation. The main parameters in the present study were the angle between the daughter ducts and the relationships between the diameters and between the lengths of the parent and daughter ducts. The performance of the branching systems was evaluated in terms of total hydraulic resistance and distribution of shear stresses. The effect of rheological parameters was also analyzed.*

These results were compared with analytical results obtained based on the Constructal Law. We show that the physical optimization in the tree-network design is not always given by a reduction of vessel size by a constant factor of $2^{-1/3}$. This type of study can be beneficial in the medical field, helping in the diagnosis and treatment of cardiac and circulatory diseases, such as in poor arterial formations and revascularization surgeries, as well as in the chemical industry, since most of the working fluids present non-Newtonian behavior.

Keywords: *Constructal design, Hess-Murray law, Y-shaped assembly, Non-Newtonian fluid.*

INTRODUCTION

Tree-shaped flow networks have been the subject of numerous investigations because of their importance in understanding the behavior of natural systems (blood vessels and bronchial tree) and the design of artificial systems. For a fluid transport system, the best flow configuration, which connects a point-to-volume or volume-to-point, is tree-shaped, and a compromise must be found between large and small ducts, as in (Bejan, 2000), (Bejan and Lorente, 2008) and (Bejan, 2017).

Assuming a Hagen-Poiseuille flow to the vascular system, (Hess, 1917) and (Murray, 1926) state that the volumetric flow rate should be proportional to the diameter cube of an optimized duct, so that the work of conducting the fluid is minimal. Therefore, optimal branching is achieved when the raised to the cube diameter of a parent vessel is equal to the sum of the cubes of the diameters of the daughter vessels. For symmetrical vessels, the relationship between diameters of daughter vessels and parent vessels is $2^{-1/3}$ (Hess-Murray law). This optimum way of connecting large and small vessels with rigid and impermeable walls is valid only as long as the flux is laminar, Newtonian, stable, incompressible and fully developed, as in the works of (Pepe et al., 2017a). However, some blood vessels and airways, among others, do not seem to follow this $2^{-1/3}$ rule. In addition, turbulent flows also do not follow this law. (Uylings, 1977) and (Bejan et al., 2000) showed that turbulent flows require an optimization rule of $2^{-3/7}$. However, the flow of fluids in living organisms is essentially laminar and the evidence suggests that exposure to turbulent flows may pose some health risk according to (Miguel, 2015).

Blood flow can be modeled as stable or pulsatile, either Newtonian or non-Newtonian. In small vessels distant from the heart, the flow can be approached as stable. In larger arterial vessels, the flow is pulsatile because of the pumping characteristics induced by the heart. Experimental studies suggest that if vessels experience high shear rates (greater than 100 s^{-1}), it is reasonable to consider blood flow as a Newtonian fluid. However, non-Newtonian effects appear at lower shear rates in vessels, such as capillaries, small arteries, and small veins. At shear rates of less than 100 s^{-1}, the blood exhibits behavior of pseudoplastic fluid, since its viscosity decreases with increasing shear rate. (Revellin et al., 2009) and (Miguel, 2016a, 2016b, 2016c) incorporates in their studies non-Newtonian rheology to reach the best way to connect large and small vessels together.

The optimization rules obtained from the minimum work principle and the Constructal Law come from 1D and 2D analytical approaches. These studies involve many assumptions and simplifications, which are based on justifications and approximations, listed in (Pepe et al., 2017b).

This article intends to obtain new knowledge about the dynamics of the flows of Newtonian and non-Newtonian fluids in bifurcated ducts, using three-dimensional numerical simulations of fluid flow in Y-shaped channels. Several geometries are treated in which it was tried to vary the dimensionless relations responsible for the construction of the same, in order to evaluate the total resistance to fluid flow (R).

The dimensionless relations used during the study were the relationships between the lengths ($\tilde{L}_1/\tilde{L}_0$), the relationships between the diameters ($\tilde{D}_1/\tilde{D}_0$), and the angle of separation between the secondary ducts (θ).

Newtonian and non-Newtonian fluids were used, the latter obeying power-law and have coefficient n of 0.78 and 1.1, being therefore of the pseudoplastic and dilating types, respectively. The Reynolds number was kept constant during the simulations and equal to 1000. Only the flow of laminar fluid, without heat transfer, was analyzed and with the walls of the pipe considered impermeable.

We sought to determine the angle values for which the total resistance to fluid flow (R) was minimized.

Similar studies were carried out by (Pepe et al., 2017b) under similar conditions, using T-shaped geometries (θ=180°) with permeable and impermeable walls. The results obtained were consistent with those found in this study.

1 METHODOLOGY

1.1 Problem description

The problem to be solved consists of the analysis of the total resistance to the flow of a set of Y-shaped conduits, in which dimensionless relations involving the lengths and diameters that characterize the geometries are varied, as well as the central angle of the Y-shaped structure.

The domain considered is three-dimensional, and only the fluid flow is analyzed, neglecting the heat transfer. The flow regime is laminar and simulations were performed under steady state with impermeable walls and the Reynolds number constant and equal to 1000. Figure. 1 shows the geometry of the problem, as well as its boundary conditions. The D_1 and D_2 dimensions are kept equal in this study, as well as the dimensions $L_1$and L_2.

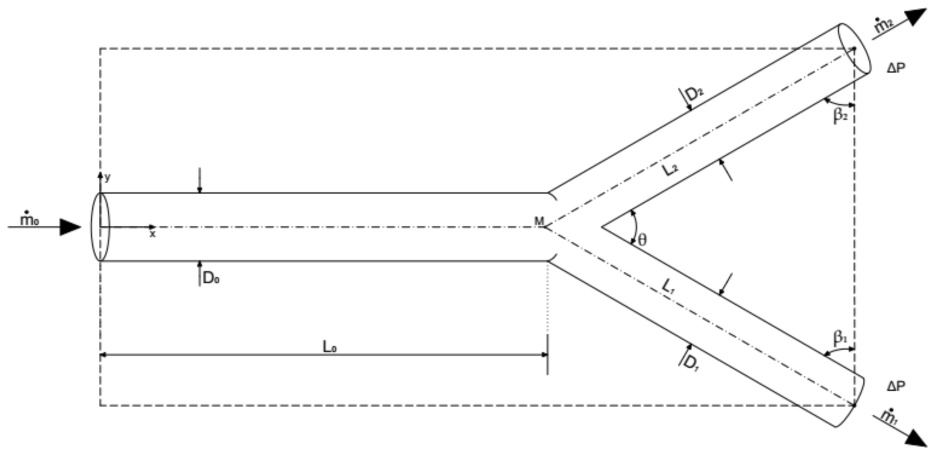

Figure 1: Representation of the computational domain and boundary conditions of the problem.

The boundary conditions of the problem are the mass flow at the duct inlet $(\dot{m}_0)$ and constant pressure at the outlet.

The method of Constructal Design was used to determine the degrees of freedom of the system, that is, the dimensions vary according to a predefined criterion. This criterion is defined on the basis of the volume of the parallelepiped circumscribed to the pipeline system, and based on the volume of the pipelines. The volume of the ducts, considering that they are much larger than the union, can be given according to Eq. (1).

$$V_D = \pi/4 \cdot \left(D_0^2 \cdot L_0 + 2 \cdot D_1^2 \cdot L_1\right) \tag{1}$$

The total volume occupied by the parallelepiped circumscribed to the ducts is given by Eq. (2).

$$V_T = A_T \cdot D_0 \tag{2}$$

Where the total area (A_T) is defined in eqs (3) to (5). L is the length of the circumscribed rectangle, and W is the width.

$$A_T = L \cdot W \tag{3}$$

$$L = L_0 + L_1 \cdot \cos(\beta) \tag{4}$$

$$W = 2 \cdot L_1 \cdot \sin(\beta) \tag{5}$$

The variables in their dimensionless forms are expressed as presented in Eqs. (6) and (7).

$$\widetilde{D}_0, \widetilde{D}_1, \widetilde{L}_0, \widetilde{L}_1 = \frac{D_0, D_1, L_0, L_1}{V_T^{1/3}} \tag{6}$$

$$\widetilde{V}_T = \frac{V_T}{V_T} = 1 \tag{7}$$

The relationship between the volume of the ducts and the volume of the parallelepiped (ϕ) was adopted as constant and equal to 0.1, and is expressed according to Eq. (8).

$$\phi = \frac{\widetilde{V}_D}{\widetilde{V}_T} \tag{8}$$

As a dimensionless parameter used to construct the geometries, the relationships between the lengths (*LR*) and the diameters (*DR*) were used, both in the dimensionless form, as presented in Eqs. (9) and (10).

$$DR = \frac{\widetilde{D}_1}{\widetilde{D}_0} = const \tag{9}$$

$$LR = \frac{\widetilde{L}_1}{\widetilde{L}_0} = const \tag{10}$$

The values used in equations (10) and (11) were first set at $2^{-1/3}$, which theoretically reduces the resistance to flow in Newtonian fluids. For non-Newtonian fluids, there are small variations of this value that minimize the resistance to flow depending on the type of fluid to be studied. The variation of the angle (θ) was performed for predetermined values, namely: 155°, 135°, 115°, 95°, 75°, 45°, 25° and 10°.

The various geometries were studied in order to establish the conditions that provide less resistance to fluid flow. Three different fluids, two non-Newtonian and one Newtonian, were used as shown in Tab. (1).

Table 1: Properties of fluids.

Fluid	Type	$\rho\,[kg/m^3]$	$K\,[Pa \cdot s^n]$	n	$\mu\,[Pa \cdot s]$
Fluid 1	Dilatant Fluid	1060	0.000147	0.78	-----
Fluid 2	Pseudoplastic Fluid	1260	0.0066	1.1	-----
Fluid 3	Newtonian Fluid	998.2	-----	1	0.001003

1.2 Mathematical and numerical formulation

The governing equations of the problem are the continuity and momentum equations in the x, y and z axis, as presented in Eqs. (11) to (14), according to (Pritchard, 2010), where ρ is the density of the fluid, u, v and w are the velocity components of $\vec{V}$ in the x, y and z directions, respectively. The viscosity is given by μ, while pressure is given by p and gravity by g.

$$\frac{\partial \rho u}{\partial x} + \frac{\partial \rho v}{\partial v} + \frac{\partial \rho w}{\partial z} + \frac{\partial \rho}{\partial t} = 0 \tag{11}$$

$$\rho \frac{Du}{Dt} = \rho g_x - \frac{\partial p}{\partial x} + \frac{\partial}{\partial x}\left[\mu\left(2\frac{\partial u}{\partial x} - \frac{2}{3}\nabla\cdot\vec{V}\right)\right] + \frac{\partial}{\partial y}\left[\mu\left(\frac{\partial u}{\partial y} + \frac{\partial v}{\partial x}\right)\right] + \frac{\partial}{\partial z}\left[\mu\left(\frac{\partial w}{\partial x} + \frac{\partial u}{\partial z}\right)\right] \tag{12}$$

$$\rho \frac{Dv}{Dt} = \rho g_y - \frac{\partial p}{\partial y} + \frac{\partial}{\partial x}\left[\mu\left(\frac{\partial u}{\partial y} + \frac{\partial v}{\partial x}\right)\right] + \frac{\partial}{\partial y}\left[\mu\left(2\frac{\partial v}{\partial y} - \frac{2}{3}\nabla\cdot\vec{V}\right)\right] + \frac{\partial}{\partial z}\left[\mu\left(\frac{\partial v}{\partial z} + \frac{\partial w}{\partial y}\right)\right] \tag{13}$$

$$\rho \frac{Dw}{Dt} = \rho g_z - \frac{\partial p}{\partial z} + \frac{\partial}{\partial x}\left[\mu\left(\frac{\partial w}{\partial x} + \frac{\partial u}{\partial z}\right)\right] + \frac{\partial}{\partial y}\left[\mu\left(\frac{\partial w}{\partial z} + \frac{\partial w}{\partial y}\right)\right] + \frac{\partial}{\partial z}\left[\mu\left(2\frac{\partial w}{\partial z} - \frac{2}{3}\nabla\cdot\vec{V}\right)\right] \tag{14}$$

The equations were solved in steady state. For non-Newtonian fluids, an apparent viscosity was calculated through Eqs. (15) and (16), as seen in (Chhabra and Richardson, 2008).

$$\tau = K \cdot \dot{\gamma}^n \tag{15}$$

$$\mu_{apparent} = K \cdot \dot{\gamma}^{(n-1)} \tag{16}$$

Where τ and $\dot{\gamma}$ are the stress and the shear rate, respectively, while k and n are the fluid consistency coefficient and the fluid behavior index, respectively.

The Eqs. (11) to (14) are solved in the FLUENT® commercial software using the finite volume method through the SIMPLE method as the coupling scheme between velocity and pressure. The Second Order Upwind was used, and the convergence criteria were established as 10^{-6} for all variables: pressure and velocity components.

2 RESULTS AND DISCUSSION

2.1 Computational model validation

The code used during the simulations was the same one used in the study by (Pepe et al., 2017b), due to the similarity of the problems. The biggest difference was the type of mesh used. While in this study polyhedral meshes were used, tetrahedral meshes were used in the one of (Pepe et al., 2017b), but the difference with the use of these two types of meshes was small (<0.42%), and due to the shorter simulation time by the use of polyhedral meshes, we opted for its use in this study.

2.2 Grid independence analysis

For the simulations polyhedral meshes were used, mainly due to the reduction in simulation time. The polyhedral meshes were made through previously existing tetrahedral meshes. Table. (2) presents the grid independence analysis. The fluid used for the study was the Fluid 1, with n = 078. The relative error between two successive meshes for the flow resistance R was used as the parameter to evaluate mesh quality.

Table 2: Grid Independence analysis.

Mesh	Elements	Nodes	$R(Pa \cdot s \cdot kg^{-1})$	$\left\lvert\frac{R^{(i)} - R^{(i+1)}}{R^{(i)}}\right\rvert$
1	34210	189626	0.283637	0.037031019
2	105382	600953	0.273133	0.024495142
3	137156	784866	0.266443	0.014518694
4	166496	952965	0.262575	0.003763932
5	231917	1332005	0.263563	----

As can be seen from Tab. (2), the mesh that presented the smallest deviation among the results was that of number 4, because of this, all the meshes used during the simulations were made with dimensions similar to this one.

2.3 Total flow resistance variation

From the results of the simulations, a graph could be drawn relating the total resistance to the flow, with the opening angle of the Y-shaped structure, for the relations ($LR = DR = 2^{-1/3}$). These relationships were chosen because they are the values that minimize the resistance of the flow, as seen in (Bejan et al., 2000). The results show that, regardless of the fluid used, the angle with the lowest resistance to flow was 135°, as can be seen in Fig. (2).

In Tab. (3) the flow resistance results for the optimal angles can be seen for each fluid studied.

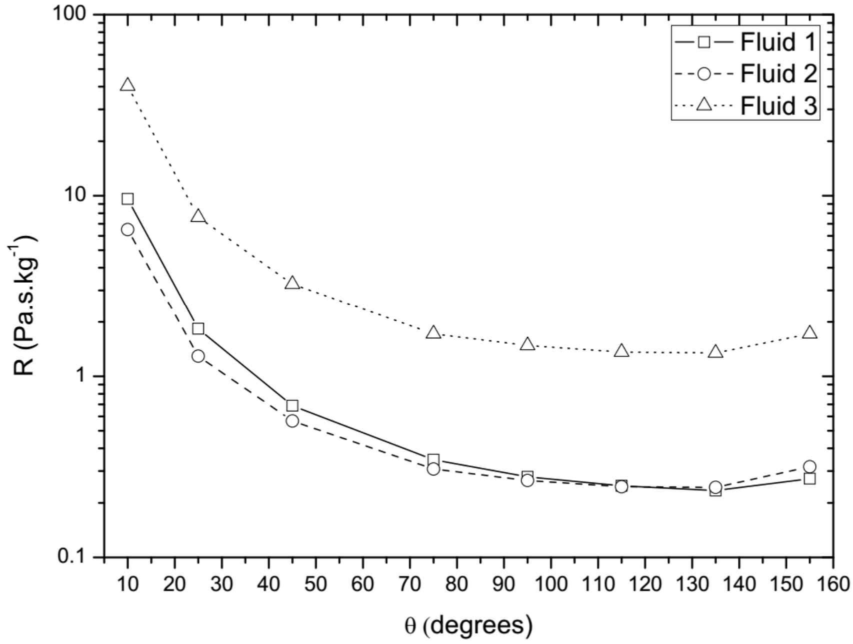

Figure 2: Resistance to flow as a function of the opening angle of Y.

Table 3: Resistance to flow at optimum angle.

Fluid	n	θ	LR	DR	$R(Pa \cdot s \cdot kg^{-1})$
Fluid 1	0.78	135°	0.8	0.8	0.234
Fluid 2	1	135°	0.8	0.8	0.243
Fluid 3	1.1	135°	0.8	0.8	1.345

The results obtained for the values of $LR = DR = 0.8$ were compared with the results obtained for the optimal ratios obtained from the Contructal Theory, namely for fluids with $n < 1$, $LR = 0.84$ and $DR = 0.77$, and for fluids with $n > 1$, $LR = 0.78$ and $DR = 0.80$, as seen in (Pepe et al., 2017a).

In the Figs. (3) and (4) it can be observed that the resistance using the optimal ratios for non-Newtonian fluids is lower than that obtained when compared to that of the optimum Newtonian fluid parameters ($LR = DR = 0.8$), however, the optimal angles remain unchanged for both fluids, and equal to 135°.

It is also interesting to note that for angles below 75°, the total flow resistance increases more abruptly, regardless of the fluid under study.

In Tab. (4) the values for the optimal angle, with the optimal dimensional relation for the non-Newtonian fluids, are summarized.

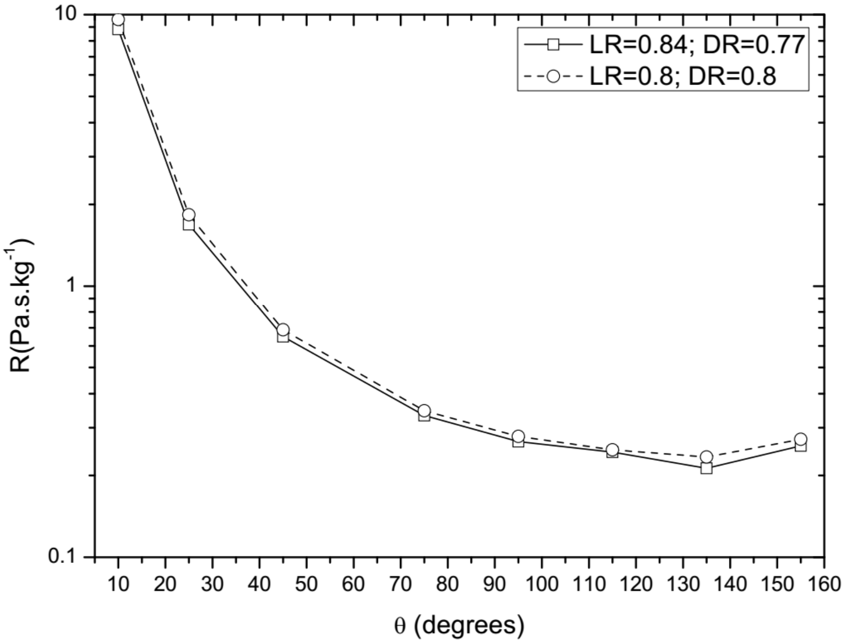

Figure 3: Resistance to flow as a function of the opening angle of Y. Fluid 1, index n=0.78.

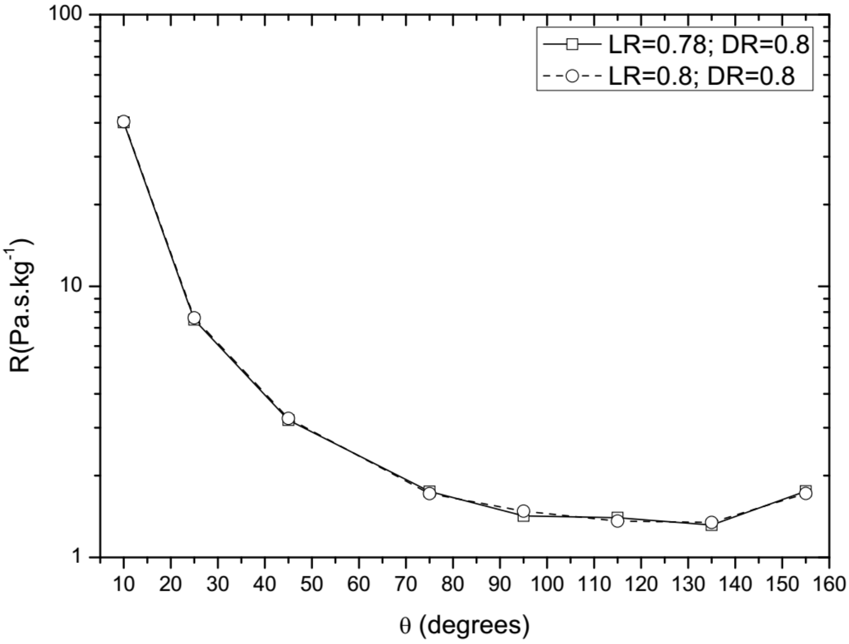

Figure 4: Resistance to flow as a function of the opening angle of Y. Fluid 3, index n = 1.1.

Table 4: Resistance to flow for the optimum angle, and optimum dimensional relationships for the non-Newtonian fluids studied.

Fluid	n	θ	LR	DR	$R(Pa \cdot s \cdot kg^{-1})$
Fluid 1	0.78	135°	0.84	0.77	0.213
Fluid 3	1.1	135°	0.78	0.8	1.315

3 CONCLUSION

The study was carried out through a series of numerical simulations with different fluid types, from Newtonian to non-Newtonian, in order to determine the angle with the lowest resistance to flow in a Y-shaped structure.

In this study, the angle with the lowest flow resistance for all fluids was the 135° angle, but it is also interesting to note that the resistance to flow increases more sharply when the angle of the Y-shaped structure is smaller than 75°.

The results were consistent with what is expected from the Constructal Theory and can be used in several areas of knowledge, from medical research to the dimensioning of pipelines used in the chemical and food industries.

ACKNOWLEDGEMENTS

This work has been partially supported by the Brazilian agencies CAPES and CNPq.

REFERENCES

Bejan, A., 2000. *Shape and Structure, from Engineering to Nature* (Cambridge University Press).

Bejan, A., 2017. Evolution in thermodynamics. *Applied Physics Reviews* 4, 011305.

Bejan, A., and Lorente, S., 2008. *Design with constructal theory*, Wiley, New Jersey.

Bejan, A., Rocha, L.A.O., and Lorente, S.; 2000. Thermodynamic optimization of geometry: T-and Y-shaped constructs of fluid streams. *Int. J. Therm. Sci.* 39, 949–960.

Chhabra, R.P., and Richardson, J.F.; 2008. *Non-Newtonian Flow and Applied Rheology*, Elsevier, 2nd edition.

Hess, W.R., 1917. Über die periphere Regulierung der Blutzirkulation. *Pflüg. Arch. Für Gesamte Physiol. Menschen Tiere* 168, 439–490.

Miguel, A.F., 2015. Fluid flow in a porous tree-shaped network: Optimal design and extension of Hess–Murray's law. *Phys. Stat. Mech. Its Appl*. 423, 61–71.

Miguel, A.F., 2016a. A study of entropy generation in tree-shaped flow structures. *Int. J. Heat Mass Transf.* 92, 349–359.

Miguel, A.F., 2016b. Scaling Laws and Thermodynamic Analysis for Vascular Branching of Microvessels. *Int. J. Fluid Mech. Res*. 43.

Miguel, A.F., 2016c. Toward an optimal design principle in symmetric and asymmetric tree flow networks. *J. Theor. Biol*. 389, 101–109.

Murray, C.D., 1926. The physiological principle of minimum work applied to the angle of branching of arteries. *J. Gen. Physiol*. 9, 835–841.

Pepe, V.R., Rocha, L.A.O., Miguel, A.F., 2017a. Is it the Hess-Murray Law always valid? *Proceedings of the Constructal Law Conference 2017,The Publishing House of the Romanian Academy, Bucharest, Romania (eds.: Morega and Lorente*), May 2017, pp. 444-455.

Pepe, V.R., Rocha, L.A.O., and Miguel, A.F., 2017b. Optimal Branching Structure of Fluidic Networks with Permeable Walls. *BioMed Res. Int*. 2017, 1–12.

Pritchard, P.J., 2010. *Fox and McDonald's Introduction to Fluid Mechanics*. John Wiley & Sons, 8th Edition.

Revellin, R., Rousset, F., Baud, D., and Bonjour, J., 2009. Extension of Murray's law using a non-Newtonian model of blood flow. *Theor. Biol. Med. Model.* 6, 7.

Uylings, H.B.M., 1977. Optimization of diameters and bifurcation angles in lung and vascular tree structures. *Bull. Math. Biol*. 39, 509–520.